AFRL-RV-PS-
TR-2013-0170

AFRL-RV-PS-
TR-2013-0170

ULTRA HIGH ENERGY DENSITY CATHODES WITH CARBON NANOTUBES

Brian J. Landi, et al.

Rochester Institute of Technology
Department of Chemical and Biomedical Engineering
160 Lomb Memorial Dr.
Rochester, NY 14604-5603

10 Dec 2013

Final Report

AIR FORCE RESEARCH LABORATORY
Space Vehicles Directorate
3550 Aberdeen Ave SE
AIR FORCE MATERIEL COMMAND
KIRTLAND AIR FORCE BASE, NM 87117-5776

DTIC COPY
NOTICE AND SIGNATURE PAGE

This report is the result of contracted fundamental research deemed exempt from public affairs security and policy review in accordance with SAF/AQR memorandum dated 10 Dec 08 and AFRL/CA policy clarification memorandum dated 16 Jan 09. This report is available to the general public, including foreign nationals. Copies may be obtained from the Defense Technical Information Center (DTIC) (http://www.dtic.mil).

AFRL-RV-PS-TR-2013-0170 HAS BEEN REVIEWED AND IS APPROVED FOR PUBLICATION IN ACCORDANCE WITH ASSIGNED DISTRIBUTION STATEMENT

//SIGNED//
DAVID CHAPMAN
Program Manager

//SIGNED//
PAUL HAUSGEN
Technical Advisor, Spacecraft Component Technology Branch

//SIGNED//
BENJAMIN M. COOK, Lt Col, USAF
Deputy Chief, Spacecraft Technology Division
Space Vehicles Directorate

REPORT DOCUMENTATION PAGE

Form Approved OMB No. 0704-0188

1. REPORT DATE *(DD-MM-YYYY)*	2. REPORT TYPE	3. DATES COVERED *(From - To)*
10-12-2013	Final Report	4 Jun 2012 – 30 Oct 2013

4. TITLE AND SUBTITLE
Ultra High Energy Density Cathodes with Carbon Nanotubes

5a. CONTRACT NUMBER
FA9453-12-1-0215

5b. GRANT NUMBER

5c. PROGRAM ELEMENT NUMBER
62601F

6. AUTHOR(S)
Brian J. Landi, Reginald Rogers, Michael Forney, and Matthew Ganter

5d. PROJECT NUMBER
8809

5e. TASK NUMBER
PPM00016746

5f. WORK UNIT NUMBER
EF008902

7. PERFORMING ORGANIZATION NAME(S) AND ADDRESS(ES)
Rochester Institute of Technology
Department of Chemical and Biomedical Engineering
160 Lomb Memorial Dr.
Rochester, NY 14604-5603

8. PERFORMING ORGANIZATION REPORT NUMBER

9. SPONSORING/MONITORING AGENCY NAME(S) AND ADDRESS(ES)
Air Force Research Laboratory
Space Vehicles Directorate
3550 Aberdeen Ave SE
Kirtland AFB, NM 87117-5776

10. SPONSOR/MONITOR'S ACRONYM(S)
AFRL/RVSV

11. SPONSOR/MONITOR'S REPORT NUMBER(S)
AFRL-RV-PS-TR-2013-0170

12. DISTRIBUTION/AVAILABILITY STATEMENT
Approved for public release; distribution is unlimited.

13. SUPPLEMENTARY NOTES

14. ABSTRACT

Free-standing carbon nanotube (CNT) electrodes were developed as suitable light-weight current collectors to effectively incorporate novel cathode nanoparticles towards high energy lithium ion batteries. The use of CNT additives with commercial high capacity lithium rich cathodes was shown to increase areal loadings and specific capacity compared to using carbon black additives. Synthesis of alternative lithium rich cathode active materials exhibited room temperature capacity of 170 mAh/g, and a high temperature capacity of 240 mAh/g. Modeling results indicate that the use of these particles coated onto CNT current collectors can result in battery energy density increases up to 15% (vs. mesocarbon microbead (MCMB)).

15. SUBJECT TERMS
Carbon Nanotubes, CNT, Ultra High Density Cathodes

16. SECURITY CLASSIFICATION OF:			17. LIMITATION OF ABSTRACT	18. NUMBER OF PAGES	19a. NAME OF RESPONSIBLE PERSON
a. REPORT	b. ABSTRACT	c. THIS PAGE			David Chapman
U	U	U	Unlimited	38	19b. TELEPHONE NUMBER *(Include area code)*

(This page intentionally left blank)

TABLE OF CONTENTS

LIST OF FIGURES

ACKNOWLEDGEMENTS

This material is based on research sponsored by Air Force Research Laboratory under agreement number FA9453-12-1-0215. The U.S. Government is authorized to reproduce and distribute reprints for Governmental purposes notwithstanding any copyright notation thereon.

DISCLAIMER

The views and conclusions contained herein are those of the authors and should not be interpreted as necessarily representing the official policies or endorsements, either expressed or implied, of Air Force Research Laboratory or the U.S. Government.

1.0 SUMMARY

This work developed free-standing carbon nanotube (CNT) electrodes as suitable light-weight current collectors to effectively incorporate novel cathode nanoparticles towards high capacity and high energy. CNTs have been shown to provide a percolation network for enhanced electron transport and mechanical stability in the cathode. The approach studied was the following: (1) process optimization of state of the art (SOA) active materials ($LiNiCoAlO_2$ (NCA)) with CNTs to produce a free-standing electrode with enhanced electron transport, and (2) development of a Li-rich layered oxide cathode to maximize capacity and increase the overall energy density of the composite matrix. Efforts in this program were also directed towards optimizing the loading of the cathode composite (i.e. thickness and CNT weight loading) through the use of CNTs as a conductive additive to improve cathode performance, specifically, the rate capability which needs to be maintained as composite thickness increases.

The first approach was to cast SOA NCA cathode composites onto CNT current collectors using an adjustable blade coater. The effect of CNT current collector purity on electrochemical performance was investigated. Coatings on as-received and unpurified CNTs were shown to have low specific capacities. However, composites coated on purified CNTs had similar performance compared to coatings on Al metal current collectors, and reach the target capacity of 185 mAh/g. The resulting mass decrease from using CNT supports results in a 5-10% increase in total cell energy density for a battery containing cathode composites on CNTs while maintaining rate capability.

The use of CNT additives with commercial high capacity lithium rich cathodes was investigated to increase areal loadings and specific capacity compared to NCA. The results demonstrated that increased weight loadings of single walled carbon nanotube (SWCNT) additives can significantly improve rate performance of higher areal capacity Li-rich composites compared to traditional composites with carbon black additives. At extremely high loadings (8 mAh/cm^2), increasing additive percentage to 2% w/w demonstrated equivalent discharge rate performance up to a C/2 rate. At the higher loadings, the rate performance may be further enhanced by optimizing ionic conductivity through controlled electrode porosity. Overall, the SWCNT additives can allow for significantly improved rate performance and higher composite areal loadings which can result in up to a 20-25% increase in battery energy density.

The second approach at increasing the cathode specific energy density was through synthesis of alternative lithium rich cathode active materials with enhanced capacity. The lithium rich cathode material synthesized reached a capacity of 170 mAh/g at room temperature and 205 mAh/g at high temperature (55°C). In order to increase capacity further, a novel technique to create lithium rich microspheres was recently pursued. The synthesis of these microspheres resulted in similar room temperature capacity of around 170 mAh/g but had a high temperature capacity of nearly 240 mAh/g which matches the commercial lithium rich material in this study. The lithium rich cathode was then coated onto a CNT current collector to further increase energy density. Lithium rich cathode materials coated onto purified CNT current collectors

demonstrated equivalent electrochemical performance. Modeling results demonstrated that the use of high capacity lithium rich cathode and CNT current collectors can result in battery energy density increases of 5-15%.

Overall, the energy density of cathodes and full batteries was demonstrated through the use of high capacity cathode materials, CNT additives, and CNT current collectors. The use of higher areal capacities was found to have the largest effect on energy density which was shown to be enabled by CNT additives. A 75% increase in energy density can be realized by moving from NCA on Al with traditional loading of 2 mAh/g to lithium rich cathodes on CNTs with an areal capacity of 8 mAh/g.

2.0 OVERVIEW OF RESEARCH, APPROACH, AND TASKS

There is a critical need for improved energy storage devices to support advancement of space power systems. Lithium ion batteries have emerged as the premier technology due to its increased energy density over other rechargeable chemistries. However, in recent years the lithium ion performance has begun to level off with incremental engineering advancements reaching a cell performance plateau of ~200 Wh/kg. The ability to double the energy density of state-of-art (SOA) lithium ion batteries requires a combined effort to increase the cathode and anode energy density. The anode has shown tremendous promise recently with nanostructured materials and CNT-enhanced free-standing electrodes, but the cathode is limited by the typical loading and active materials. The next transformation in cathode technology needs to be alternative approaches to electrode design and the use of nanostructured materials. Thus, it would be a transformational development to develop a cathode system which combines a high capacity active material (e.g. $x\mathrm{Li_2MnO_3}$-(1-x) $\mathrm{LiMn_{0.33}Ni_{0.33}Co_{0.33}O_2}$ due to its high capacity potential: > 200 mAh/g) with an alternative light-weight carbon nanotube (CNT) current collector.

The proposed research plan was to develop an ultra-high energy cathode which demonstrated reversible cycling at a high electrode loading (8 mAh/cm^2), and sufficient rate capability for space battery applications involving prismatic form factors. Each of these goals was pursued using highly conductive, light-weight CNT current collectors. The overarching objective was to increase both energy and power density through a novel CNT-enhanced design without compromising safety and cycle life over SOA. The following is a summary of the tasks pursued during this program:

Task 1: *Investigate coating of CNT current collectors with conventional cathode composites containing materials like $LiCoO_2$ and $LiNiCoAlO_2$. Evaluate the use of CNTs as conductive additives in composites as a function of composite thickness. Measure the lithium ion capacity and rate capability.*

Task 2: *Develop synthesis of high energy lithium rich metal oxides. Evaluate the use of CNTs as conductive additives in composites as a function of thickness on a conventional aluminum current collector. Measure the lithium ion capacity and rate capability.*

Task 3: *Assess the combined improvements of Tasks 1 and 2 to enhance the cathode energy density. Measure the lithium ion capacity and rate capability of novel CNT-based electrodes.*

3.0 INTRODUCTION

The energy density of battery electrodes can be increased by using a free-standing CNT paper as a current collector replacement, where the composite slurries would be coated onto CNT papers, or form a free-standing composite, where the active materials and CNTs are mixed and coated or filtered to form a three-dimensional composite. In either case, the increase in energy is due to the complete elimination of the current collector. Previous studies have looked at using CNTs as current collectors with next generation materials, such as Si, Ge, and vanadium, but there have been few studies investigating the energy density gains using CNTs as current collectors with today's SOA materials[1, 2].

In order to quantify an impact on energy density, the specific capacities of the active cathode material, $LiNiCoAlO_2$ (NCA), were modeled and compared to the total electrode specific capacities including the current collector, binder, and conductive additive at different areal loadings. The total electrode specific capacity gives a much more accurate indication of the actual effect on energy density of a full battery because all of the components of the electrode are included. Figure 1 compares the specific capacity of NCA material to electrode specific capacity when coated on Al foil or CNT papers.

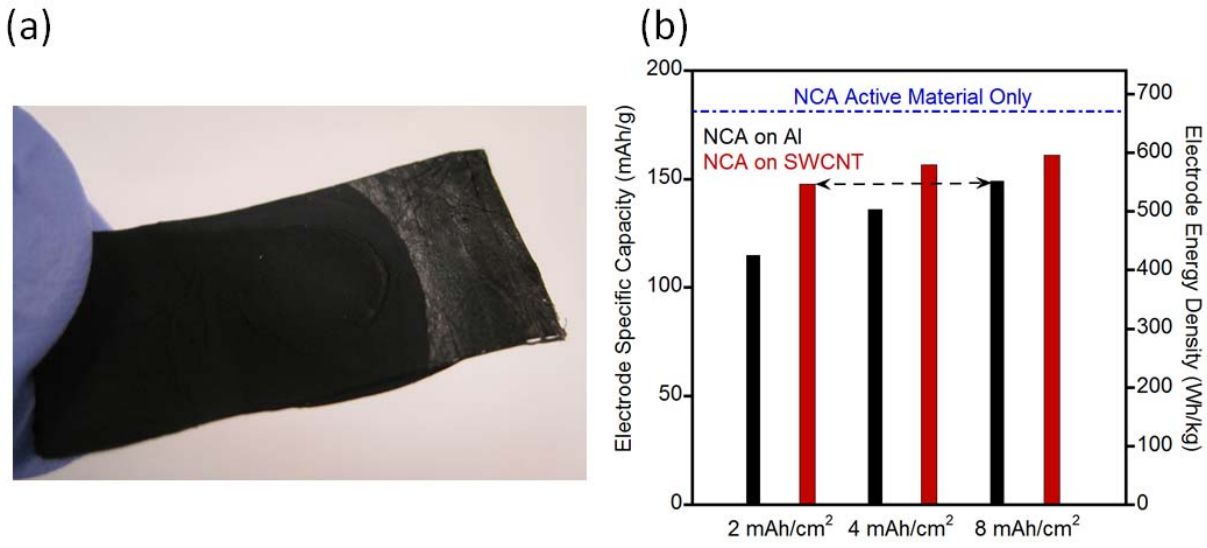

Figure 1. (a) Carbon nanotube paper coated with NCA cathode composite for testing as positive electrode in Li-ion battery (b) Comparison of NCA specific capacity (blue dotted line), NCA coated on Al (black) and NCA coated on CNT (red) specific capacity and electrode energy density as a function of areal electrode loadings 2, 4, and 8 mAh/cm^2

The specific capacity of the NCA material is the same for either current collector since this is the active material capacity around 185 mAh/g regardless of the current collector used. As the areal electrode loading is increased from 2 to 8 mAh/cm^2 the relative mass of the current collector is decreased thus increasing electrode energy density. However, the CNT paper is a lower percentage of the total electrode mass to begin with therefore the change in electrode capacity with loading isn't as significant. By using the CNT paper as the current collector, a 28% improvement in electrode capacity is found at the standard loading of 2 mAh/cm^2 and has only a slight improvement at higher 8 mAh/cm^2 loadings of 8%. Equivalent electrode energy densities can be reached with a 2 mAh/cm^2 coating on SWCNTs versus an 8 mAh/cm^2 coating on Al allowing for a thinner coating which improves power capability simultaneously.

The effect of CNT paper properties such as, purity, conductivity, and CNT type on current collector performance is not well understood. The purity of CNT materials can typically be related back to the performance of the material in a variety of devices, and is dependent on synthesis method and post-processing. The presence of metallic impurities may cause undesirable side reactions or be corroded when used as a current collector. The conductivity of CNT papers can vary significantly with CNT type (e.g. single, multi, double wall CNTs), alignment, and processing (doping, densification) [3, 4]. Currently, high conductivity bulk CNT papers are an order of magnitude lower in conductivity to copper, but have reached conductivity values equal to that of titanium which is a common lithium ion battery current collector[5]. This study investigates using commercially available CNTs as current collectors for traditional lithium ion battery electrode composites. A purification technique was developed to determine the effect of purity on current collector performance.

There exists a number of ways to improve the energy density of a lithium ion battery. Energy density is typically stated in terms of Wh/kg which is the energy provided by the active materials (the materials shuttling lithium ions) divided by the entire mass of the battery which includes packaging, electrolyte, current collectors, binders, and conductive additives. Increases in energy density can be made by decreasing component masses and/or increasing the energy of the battery by changing active material loading or structure.

The majority of research to improve energy density has focused on increasing the active materials capacity and/or voltage. However, the state-of-the-art commercial cathode capacity is still only between 180-200 mAh/g which is lower than the standard anode which has a capacity around 300-330 mAh/g. Therefore, in order to capacity match the electrode, a higher cathode capacity and/or loading is needed which lowers the battery energy density. Recently, a higher capacity lithium rich cathode material which can reach 250-300 mAh/g was discovered that can better match high capacity anodes. However, higher loadings may still be necessary to match higher capacity Si and Ge anode materials. At higher loadings, a percolation network is more difficult to form, and a new additive may be needed to achieve sufficient performance. Therefore, lithium rich cathodes with CNT additives were investigated at varying areal capacities and compared to standard additive formulations.

Lithium rich cathode materials with high capacities of 250-300 mAh/g where only recently discovered and are scarcely available commercially. Therefore, the lithium rich materials were

synthesized in house to obtain the high capacity material following the procedure published by Argonne National Laboratory, and investigate if any improvement could be made[6].

The NanoPower Research Labs (NPRL) is also testing an alternative high capacity layered lithium-rich metal oxide cathode, which was reported to be a hollow $0.3Li_2MnO_3 \bullet 0.7LiNi_{0.5}Mn_{0.5}O_2$ microsphere product with reversible capacities up to 295 mAh/g.[7] The data that was reported shows stable cycling for 100+ cycles, as well as good rate performance up to 2-5C at room temperature. Cycling performance was also shown to be stable at 55 °C, with a small reduction in capacity.

The combination of high capacity lithium rich cathode materials coated onto light weight CNT current collectors can significantly increase electrode energy density, and more optimally match higher capacity anode materials. The highest capacity cathode material in this study was the commercial lithium rich material from NEI which had a room temperature capacity of 206 mAh/g and a high temperature (55°C) capacity of 240 mAh/g. This work also demonstrated the importance of CNT purity on current collector performance to obtain the desired capacity while reducing mass. Therefore the commercial NEI Li-rich cathode was coated onto a purified CNT current collector to obtain the highest electrode energy density.

4.0 METHODS, ASSUMPTIONS, AND PROCEDURES

Electrode slurries were prepared by combining the electrode materials with N-Methyl-2-pyrrolidone (NMP) and mixing in a THINKY ARE-310 planetary centrifugal mixer at 2000 rpm. The slurries were coated onto commercial CNTs (Nanocomp AA-0043) using a RK Control Coater 101 with adjustable spreading blade applicator, and dried subsequently at 80°C for 1 hour. Coatings on as-received and purified Nanocomp CNTs were compared. The CNT sheet was burned in air to 560 °C at a 10 °C min^{-1} ramp rate, and resulted in a >50% w/w reduction in the mass of the CNT sheet material. A concentrated HCl (37.5% w/w HCl in H_2O – Sigma Aldrich) rinse was used to remove the particles on the surface where the CNT sheet was allowed to soak for an additional 15 minutes with slight agitation before being rinsed with DI H_2O for 30 minutes. The CNT sheet was then dried in a vacuum at 100 °C overnight. The slurries were mixed at a mass ratio of 92 wt % Cathode ($LiNiCoAlO_2$ or $Li_2MnO_3 \bullet LiNiMnO_2 \bullet LiNiMnCoO_2$ (Li-rich) (NEI Corporation), 4 wt % KYNAR Powerflex polyvinylidene fluoride (PVDF), and 4 wt % Super P (Timcal) in NMP for the cathode. Cathode slurries integrating SWCNTs as a conductive additive replacement were mixed with 4% PVDF binder for all sample and the amount of active material was adjusted for the percentage SWCNTs used (95NEI:1SWCNT,94NEI:2SWCNT). The SWCNT material used in the current study was produced through laser vaporization and purified to the equivalent of the "100%" reference standard as in previous work[8]. The slurry containing SWCNTs was formed by alternating bath ultrasonication (38.5-40.5 Hz at 40°C) and planetary centrifugal mixing of the SWCNTs in NMP and PVDF solution to improve the dispersion and final mixing with Li-rich cathode. The ratio of concentration of SWCNTs in NMP (mg/mL) was kept constant to ensure proper SWCNT dispersion, and the height of the adjustable blade coater was adjusted to obtain the desired areal loading. Each composite electrode was then vacuum-dried at 100°C and compressed using a chrome coated roller (MTI Corp.).

The electrodes were galvanostatically cycled using an Arbin BT-2000 at 25°C vs. Li/Li^+ cell using a lithium metal foil in a 2032 coin cell configuration. The electrolyte was 1.2M $LiPF_6$ in ethylene carbonate (EC) and ethyl methyl carbonate (EMC) at a ratio of 3:7 by volume, respectively. The analysis of capacity as a function of rate was performed between 2.5 - 4.3V for NCA cathode electrodes and 2.0-4.6V for Lithium rich materials. The analysis of capacity as a function of rate was performed between 2.5 - 4.6V vs. $(Li/Li^+)/V$ with a constant voltage step at 4.6V until the current dropped to 10% of the original current. The charge rate was at C/10 for the first cycle, and was a C/5 rate for subsequent cycles. The discharge rate was then adjusted at varying rates (C/10, C/5, C/2, 1C). Scanning electron microscopy was performed using a field emission Hitachi S-900 microscope at 2kV. X-ray diffraction (XRD) measurements were performed with a D2 Phaser benchtop XRD system (Bruker AXS, Germany) using Co Kα radiation (k=1.789 A˚) scanning between 2θ of 10° and 80°. All samples were prepared by uniform packing of material in sample holders.

Differential Scanning Calorimetry (DSC) measurements were performed using a TA Q100 DSC, and heating at a rate of 10°C/min under a nitrogen purge. Samples were prepared by charging half cells to 4.6V vs. $(Li/Li^+)/V$ after a complete charge-discharge cycle and a constant output potential difference float charge at 4.6V for 12 hours to delithiate the lithium rich cathode. The electrodes were removed from the coin cells in an argon-filled glove box, and sealed in an aluminum DSC can for testing. The specific exothermic energy released ($J\ kg^{-1}$) was calculated by integrating under the main peak based upon the heat flow data normalized to the active cathode material mass. Triplicate samples were analyzed to account for any slight variations in coating, electrolyte uptake, and sample preparation.

Lithium-rich metal oxide cathode active materials were prepared following synthesis first reported at Argonne National Lab [6]. Briefly, nitrates of cobalt, nickel, and manganese were dissolved in deionized water. To facilitate the dissolution and reaction, the aqueous solution was heated to 50°C. To the solution, ammonium hydroxide was added to raise the pH to 11. After two hours of mixing, the solution became brown in color at which point it was removed from heat. The solution was filtered using a vacuum filtration unit to collect the precipitate. The precipitate was heated to 400°C in a muffle furnace for 4 hours to dry the material. Afterwards, excess lithium hydroxide was added to the powder and further annealing at 900°C for 4 hours was completed. After annealing, the final product was stored for characterization and testing.

Figure 2. Synthesis process for production of Li-rich metal oxide cathode material

NPRL has been following the procedure outlined in the literature,[7] and is working towards achieving the reported specific capacities. The first step of the procedure is to mix $MnSO_4 \cdot H_2O$ in 700 mL deionized (DI) water and, separately, NH_4HCO_3 in 700 mL DI water. These two solutions are then mixed together with 70 mL of ethanol and stirred for 2 hours at room temperature to synthesize $MnCO_3$ microspheres (Figure 3a). After mixing the precursors to form $MnCO_3$ microspheres, the microspheres are collected by vacuum filtration onto a 1 µm pore size filter (Figure 3b). The harvested $MnCO_3$ microspheres are then stored under vacuum overnight at room temperature to dry. The size and structure of the NPRL synthesized $MnCO_3$ microspheres are shown in Figure 4a. It should be noted that NPRL synthesized microspheres have a mean diameter of 1.5 µm, whereas the literature scanning electron microscope (SEM) suggest a size of 3-5 µm. Figure 4b presents an XRD spectrum of the $MnCO_3$ microspheres that matches the expected spectrum, which is indicated by the blue bars and dashed vertical lines.

The next step in the process is to convert the $MnCO_3$ microspheres into MnO_2 microspheres by a 5 hours thermal treatment at 400 °C, which we do in a Carbolite HTR 11-75 Rotary Reactor Furnace (Figure 3c). The literature suggests a ramp rate of 1 °C/min, and we have tested both 1 °C/min and 5 °C/min with compressed air flowing over the microsphere powder.

Next the MnO_2 microsphere powder is dispersed into 100 mL ethanol with $LiOH \cdot H_2O$ and $Ni(NO_3)_2 \cdot 6H_2O$. The literature procedure calls for evaporating the 100 mL of ethanol by heating to 50 °C, and evaporating to dryness. The resulting powder is then ground in an agate mortar and pestle for 30 min. In order to conserve ethanol and minimize the amount of solvent sent up the fume hoods, alternative methods are being tested, such as dispersing in water, using a rotary evaporator, or solvent recovery with a condenser.

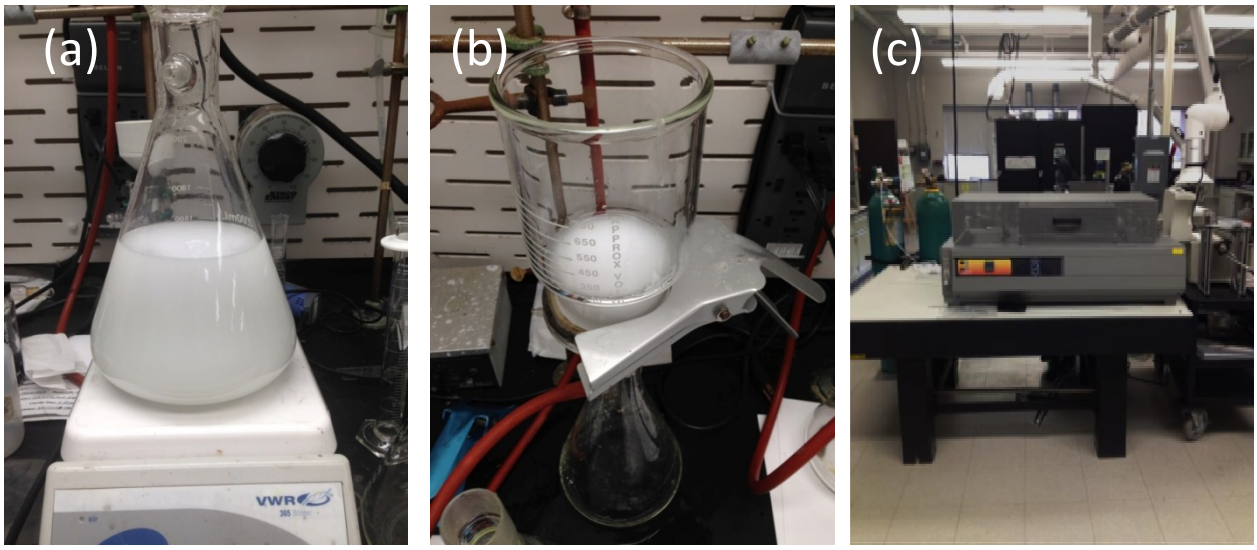

Figure 3. (a) solution based synthesis of $MnCO_3$ microspheres, (b) filtration to collect $MnCO_3$ microsphere product, and (c) rotary furnace that is used for conversion of $MnCO_3$ to MnO_2 and sintering to form the hollow $0.3Li_2MnO_3•0.7LiNi_{0.5}Mn_{0.5}O_2$ microspheres final product

The final step is to sinter the powder at 800 °C for 10 hr. According the literature, this step allows the Li/Ni salts to react with the porous MnO_2 microspheres, resulting in $0.3Li_2MnO_3•0.7LiNi_{0.5}Mn_{0.5}O_2$ microspheres. It is suggested that fast outward diffusion of Mn/Ni atoms and slow inward diffusion of O atoms, through the Kirkendall effect, is what causes the hollow structure.

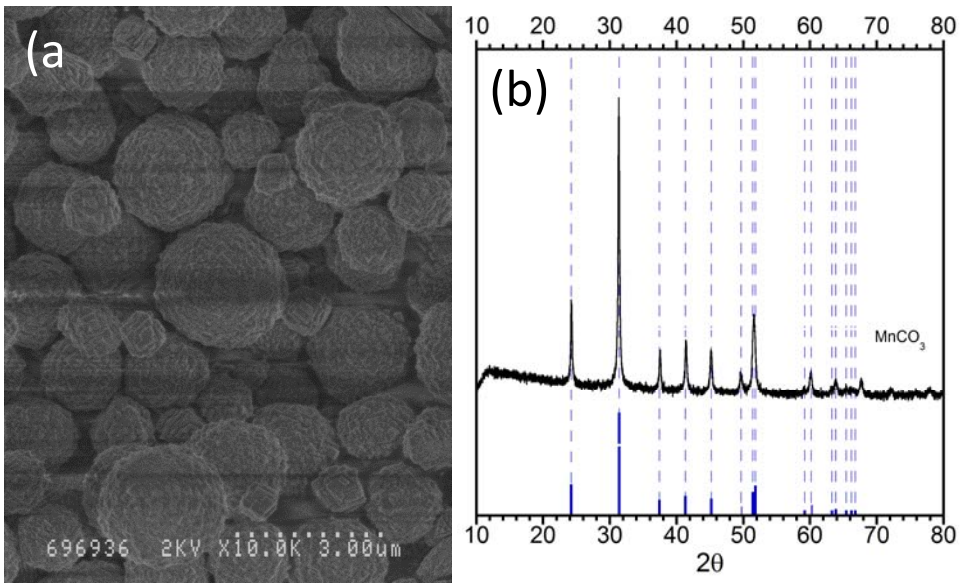

Figure 4. (a) NPRL synthesized $MnCO_3$ microspheres and (b) XRD spectrum of NPRL synthesized $MnCO_3$ microspheres

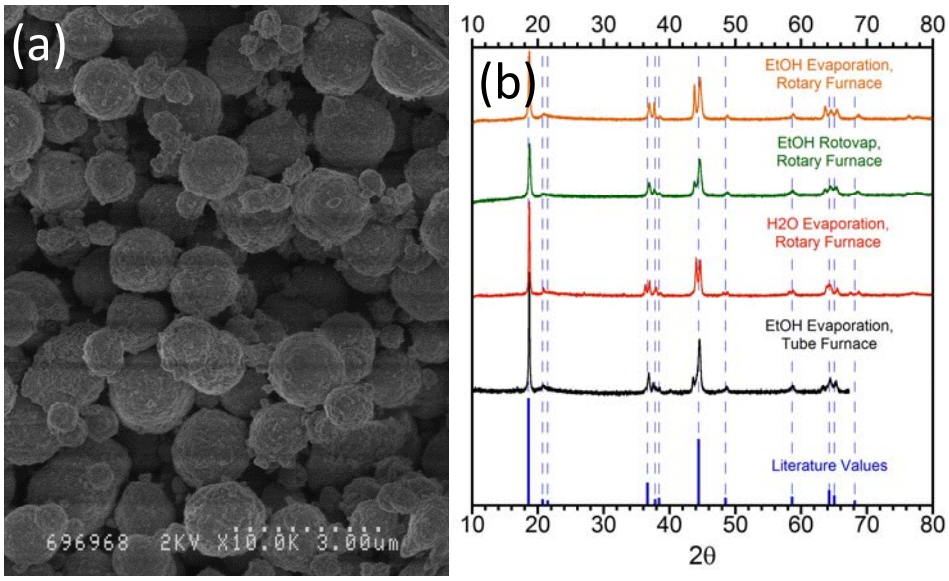

Figure 5. (a) SEM image of NPRL synthesized $0.3Li_2MnO_3 \cdot 0.7LiNi_{0.5}Mn_{0.5}O_2$ microspheres final product and (b) XRD spectra of the final product under several synthesis conditions

Figure 5(a) is an SEM image of NPRL synthesized $0.3Li_2MnO_3 \cdot 0.7LiNi_{0.5}Mn_{0.5}O_2$ microspheres. Figure 5(b) has several XRD spectra from synthesis runs where the ethanol evaporation protocol has been varied. All cases show promising agreement with the expected XRD spectrum, though some of the peaks exhibit splitting that may indicate a subtle problem with the crystal structure.

Microsphere electrodes were fabricated from the $0.3Li_2MnO_3 \cdot 0.7LiNi_{0.5}Mn_{0.5}O_2$ microspheres with an 80:10:10 ratio of active:PVDF:SuperC, made into a slurry with NMP, and blade-coated to get cathodes with a composite thickness of approximately 50 μm. Cathodes are punched out of the electrode composite, and then assembled into coin cells for electrochemical testing vs. lithium. The literature called for an electrolyte solvent mixture of EC:DMC, but this solvent mix does not wet our Celgard separators well, so we have tested our coin cells with our standard EC:EMC.

5.0 RESULTS AND DISCUSSION

5.1 CNT Current Collector

Purification methods were investigated for commercial Nanocomp CNTs. As seen in Figure 6(a), the as-received CNTs contain a significant amount of carbonaceous and metallic impurities. Initial attempts of purification followed techniques described previously that are used to purify SWCNTs where the CNT paper is refluxed in a nitric acid and HCl bath to remove metallic impurities. The paper is then thermally oxidized to remove non-CNT carbonaceous impurities. This process did not significantly improve the CNT paper purity. As can be seen in the photograph inset in Figure 6(a), even when the paper is exposed to concentration HCl no reaction or metallic dissolution occurs. This is most likely due to carbon coating the metallic particles and preventing dissolution. Therefore, the CNT paper was first thermal oxidized as seen in

Figure 6(b). The high temperature burn appears to have removed the carbonaceous impurities but the metal is still present. When the burned paper is placed in concentrated HCl, a solution color change is instantly visible due to metallic dissolution. After neutralizing the paper with water rinses, the purified paper is absent of both metallic and carbonaceous impurities as observed in Figure 6(c).

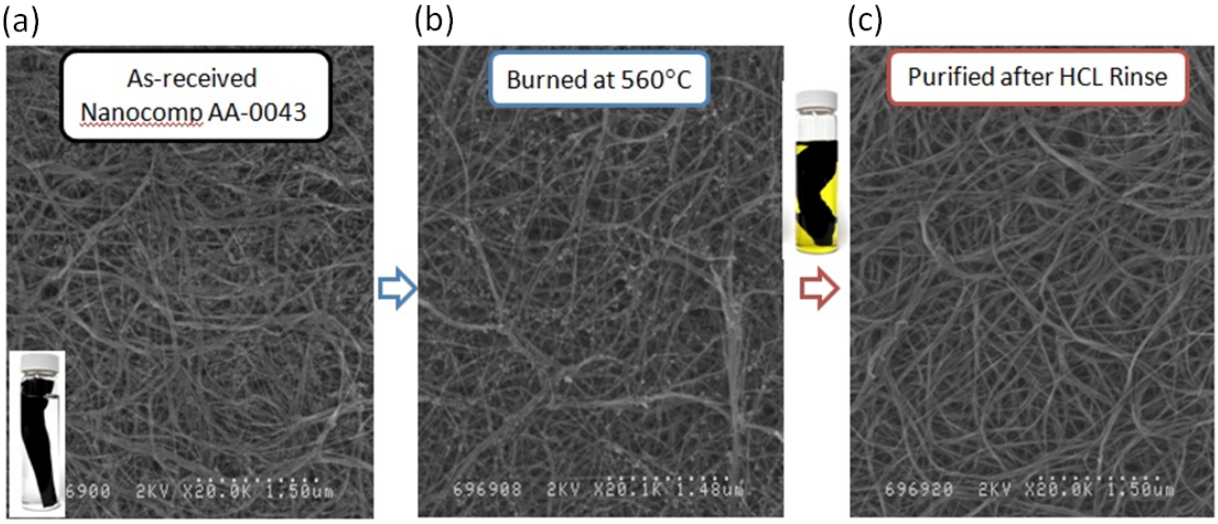

Figure 6. (a) As-received Nanocomp paper purification through (b) thermal oxidation and (c) concentrated HCl rinse. The photograph inset in (a) is as-received CNTs in concentrated HCl (no reaction), and the photograph between (b) and (c) is CNT paper after thermal oxidation in concentrated HCl (metal dissolution)

Previous work with anode coatings mesocarbon microbead (MCMB) based) on CNT current collectors demonstrates the ability and benefits of coating onto a CNT electrode. Cross sectional SEM images of a cleaved MCMB composite coated on purified CNTs can be seen in Figure 7 with increasing magnification. The images show a uniform CNT paper that is compliant with the composite and can compress to provide enhanced contacting. Even in areas that became delaminated due to electrode cleaving, the SWCNTs can be seen bridging the gap between the CNT paper and the composite in the higher magnification image. Therefore, a CNT paper may be able to provide electrical contact even after partial composite delamination.

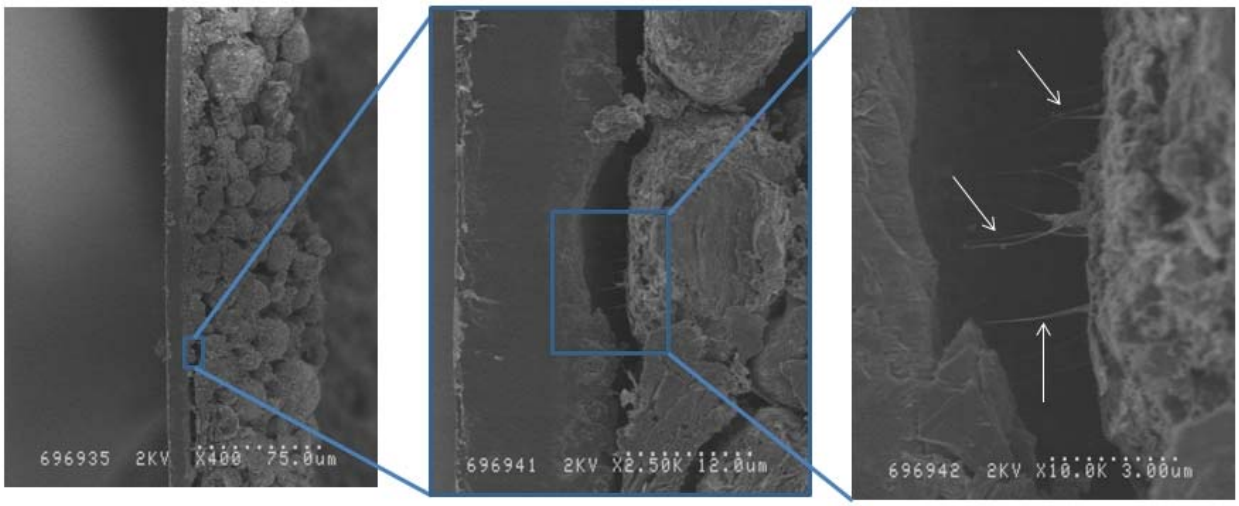

Figure 7. Cross-sectional images of example MCMB composite coated on CNT paper with increasing magnification

Evaluation of purified CNT sheets to support a standard cathode composite consisting of $LiNi_{0.8}Co_{0.15}Al_{0.05}O_2$ (NCA), PVDF binder, and carbon black has been performed. Although the mass savings is less significant than on the anode with a Cu current collector, the CNTs are still less dense than Al current collectors and improve energy density as previously discussed. The use of CNTs as a cathode current collector should not have the issue of excess SEI formation and first cycle loss as the CNTs are anodic in nature and SEI formation on the cathode isn't as significant. The electrochemical results shown in Figure 8 demonstrate the ability to use CNT current collectors on the cathode as well. The purity of the CNT current collector is shown to be important to reach the desired electrochemical performance. The cathode composite coated on the as-received CNT sheet has a significantly lower capacity of around 150 mAh/g. Whereas, the specific active capacity was measured to be around 185 mAh/g for NCA coated onto purified CNT and Al current collectors, which is standard for NCA composites. The coulombic efficiency for purified CNT sheets is demonstrated to be comparable to composites coated on Al foil. The rate capability of NCA composites on Al and purified CNT current collectors was measured at increasing discharge rates. The cycling and capacities were similar with the composite on CNTs having a slightly higher capacity demonstrating that CNT current collectors can provide equivalent rate performance to Al.

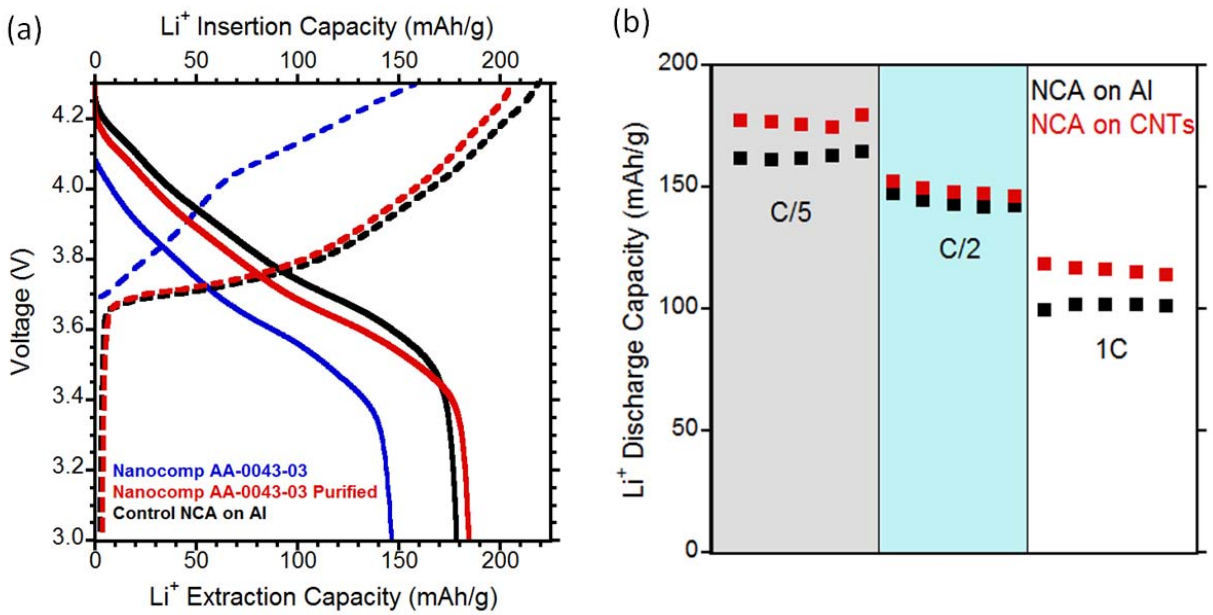

Figure 8. (a) Charge-discharge capacities for Al and as-received and purified CNT electrodes coated with NCA cathode composite. (b) Discharge capacities as a function of rate and cycle for NCA on Al and purified CNT paper. Each rate was held for five cycles

5.2 CNT Additives and Lithium Rich Cathodes

Lithium rich cathode material was purchased from NEI Corporation and characterized through x-ray diffraction and scanning electron microscopy. XRD results show that the material is a mixture of Li_2MnO_3, $LiNiMnO_2$, and $LiNiMnCoO_2$ as demonstrated in Figure 9. The SEM images demonstrate that the NEI Li-rich cathode material is of uniform size with particles on the order of 0.5-1.0 μm.

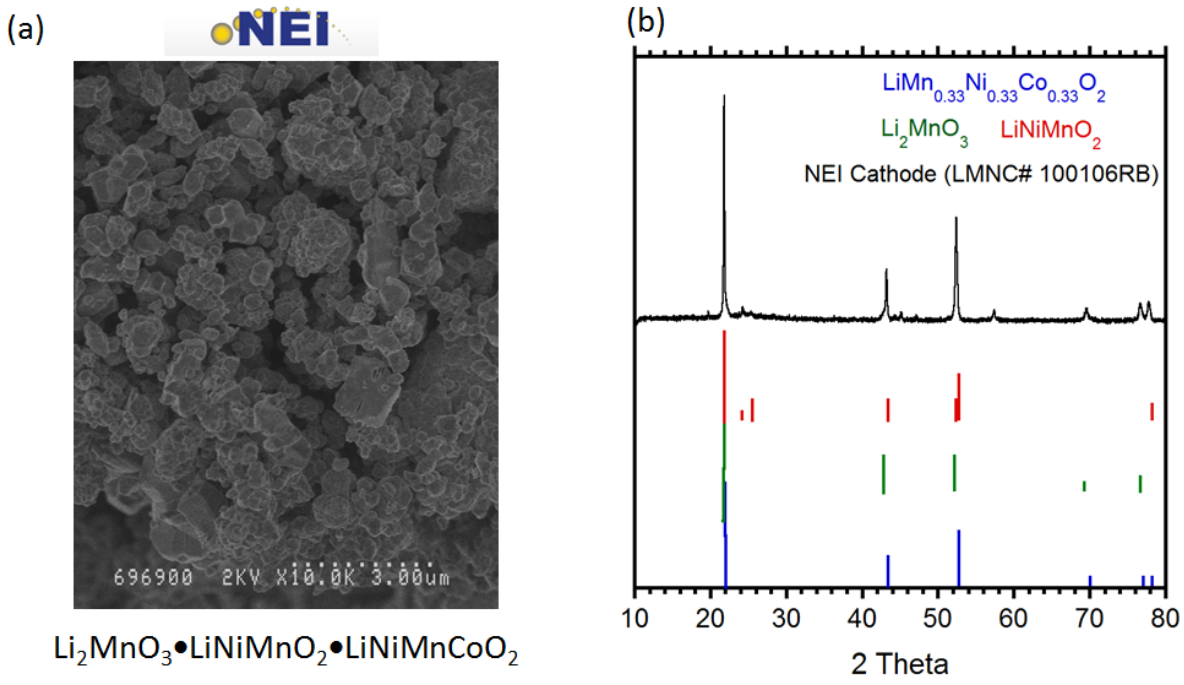

Figure 9. (a) Scanning electron microscopy image of commercial lithium rich NEI material at magnification of 10,000x. (b) X-ray diffraction of commercial lithium rich NEI material with the respective reference lines

Typical areal loading capacities for commercial lithium ion battery electrodes are around 2 mAh/cm^2, and go as high as 4 mAh/cm^2. Batteries containing higher areal loadings are considered for energy density only and are used for applications that allow for slow charge-discharge rates. At faster discharge rates, a higher voltage drop and lower capacity is found due to resistive losses caused by a thicker low conductivity composite. SWCNTs have been shown to improve rate capability and conductivity of composites previously at a low loading of 1%[9]. However, a higher percentage of SWCNTs may be necessary to improve the rate performance of thicker and higher areal loading electrodes. A Li-rich commercial cathode composite at a loading of 4 mAh/cm^2 with 4% carbon black additive vs. 1.0 and 2% SWCNT additive is shown in Figure 10. Previous work compared 1% SWCNTs with 4% carbon black at a low loading of ~1.6 mAh/cm^2, and demonstrated similar capacities up to a 2C rate with the SWCNT composite having higher capacity and voltage retention at 5C and 10C rates. However, at a higher areal loading of 4 mAh/cm^2 a higher capacity and average voltage was found starting at a 1C rate. This demonstrates the importance of composite conductivity at higher areal loadings. When the weight loading of SWCNT additive is increased further, a higher capacity and average voltage was measured.

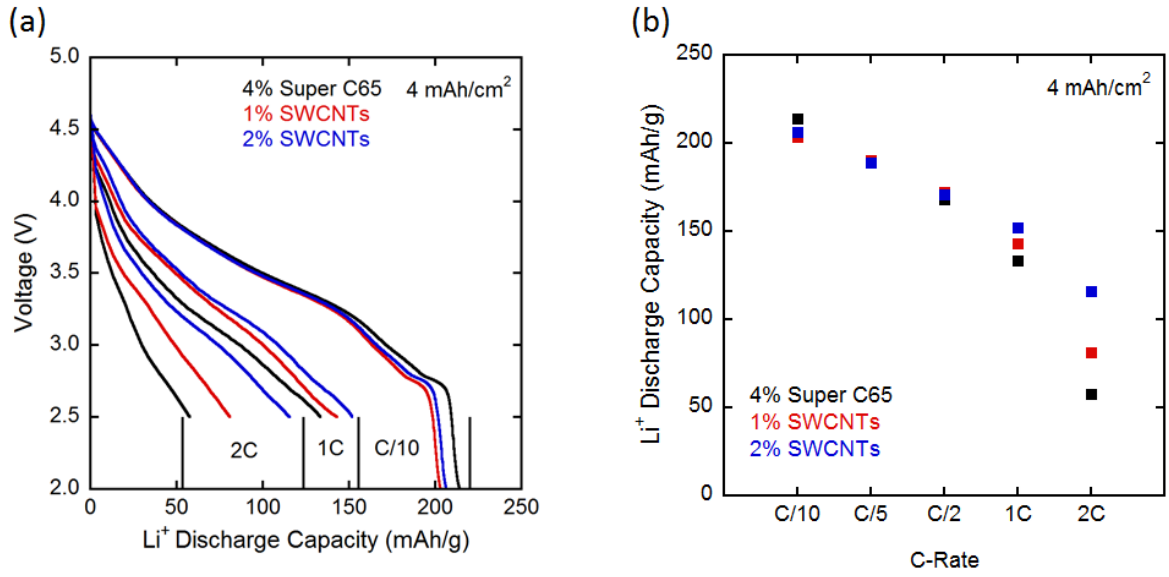

Figure 10. (a) Voltage discharge curves at increasing discharge rates of commercial NEI lithium rich cathode with standard additive (4% Super C65 carbon black) and 1% and 2% SWCNT additive at a loading of 4 mAh/cm^2. (b) Comparison of discharge capacities at varying discharge rates for NEI cathode with standard and SWCNT additives

Composites were made at an areal loading of 8 mAh/cm^2 to further increase electrode energy density and determine the effect of the additive on performance. At higher areal capacity loadings (thicker composites), the results demonstrate the necessity for a higher SWCNT loading to maintain capacity at modest rates.

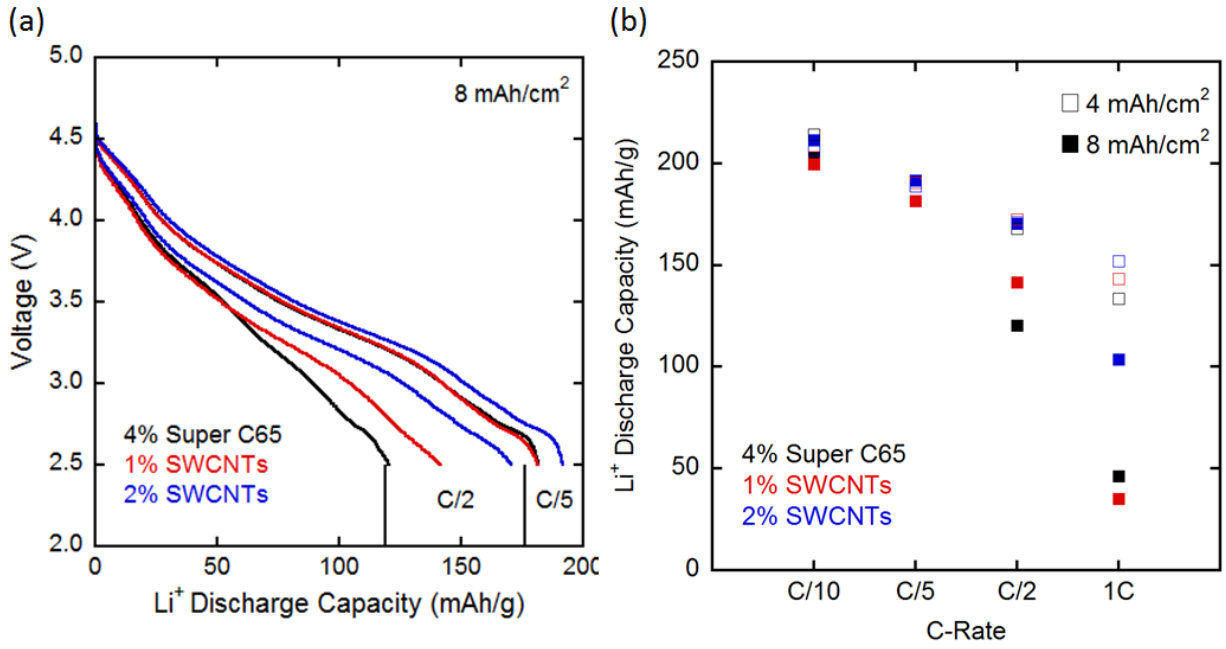

Figure 11. (a) Voltage discharge curves at increasing discharge rates of commercial NEI lithium rich cathode with standard additive (4% Super C65 carbon black) and 1% and 2% SWCNT additive at a loading of 8 mAh/cm^2. (b) Comparison of discharge capacities at varying discharge rates for NEI cathode with standard and SWCNT additives at 4 and 8 mAh/cm^2 loadings

Differential scanning calorimetry was measured for the 4 mAh/cm^2 loading composites in Figure 12 that were fully charged, removed from coin cells, and placed in DSC pans to determine the effect of the additives on thermal stability. DSC runs were performed under nitrogen at a heating rate of 10°C/min. The exothermic energy release (J/g) was calculated by integrating under the peaks. DSC results show a slight decrease in exothermic energy release and peak intensity by using SWCNT additives thus demonstrating an improvement in composite thermal stability consistent with previously published results.

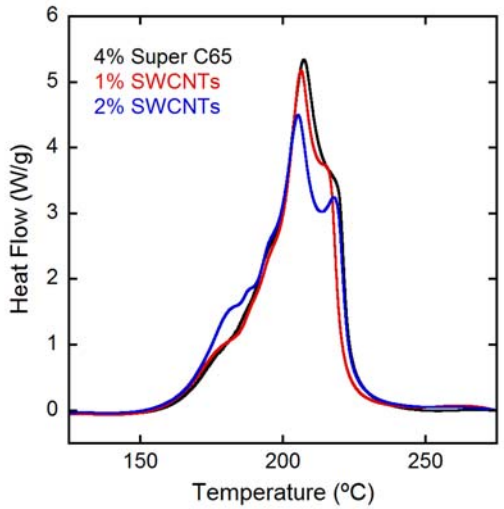

4% Super C65 – Exothermic Release – 844 J/g
Peak Intensity – 5.34 W/g

1% SWCNTs – Exothermic Release – 773 J/g
Peak Intensity – 5.17 W/g

2% SWCNTs – Exothermic Release – 812 J/g
Peak Intensity – 4.5 W/g

Figure 12. Differential scanning calorimetry of de-lithiated commercial NEI lithium rich cathode with standard additive (4% Super C65 carbon black) and 1% and 2% SWCNT additive at a loading of 4 mAh/cm^2

5.3 Lithium Rich Cathode Synthesis

Scanning electron microscopy (SEM) images were taken of the as-synthesized material to characterize the morphology and surface structure. Figure 13 shows representative SEM images of Li-rich material synthesized with x set at 0.1 (a), 0.3 (b), and 0.7 (c). The SEM images indicate nanocrystalline material most achievable when x = 0.3. For the other x values synthesized, particle sizes are greater than 1 mm as shown in Figure 13. Based on this qualitative assessment, x = 0.3 is chosen as the focus for all subsequent temperature and pH studies during synthesis.

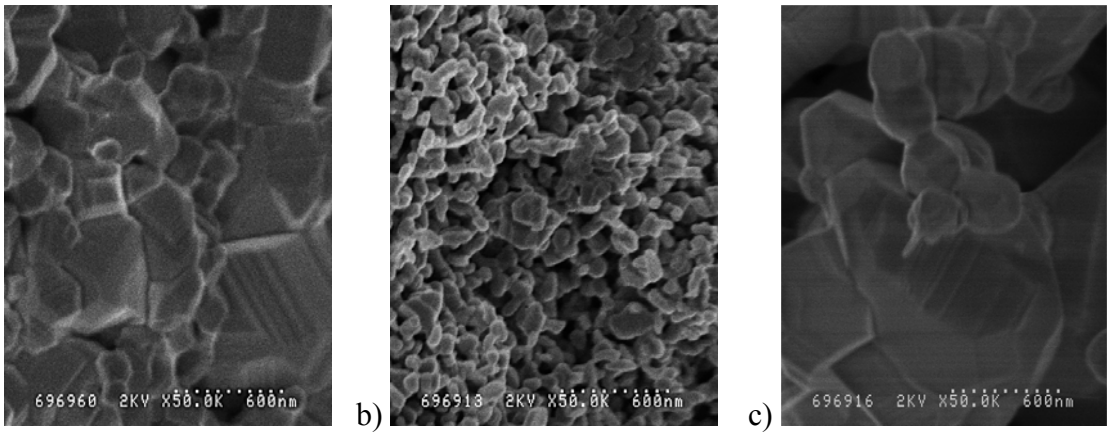

Figure 13. Scanning electron microscopy images of xLi_2MnO_3-(1-x)$Li(CoMnNi)_{0.33}O_2$ cathode active materials synthesized with x equal to (a) 0.1, (b) 0.3, and (c) 0.7

Initial synthesis of the Li-rich material showed a large degree of variability in the resulting product attributed to a wide control of the temperature and pH of the solution. To determine if tighter control over the temperature and pH parameters would facilitate an improvement in the quality of the material, more stringent control over the temperature and pH during synthesis was implemented. SEM characterization of moderate and stringent control is shown in Figure 14. Analysis of the SEM images shows that stringent control of pH and temperature parameters lead to smaller particle size and more crystalline material. This smaller particle size is believed will translate to better electrochemical performance when tested in a coin cell opposite a reference anode (i.e. Li metal).

(a) 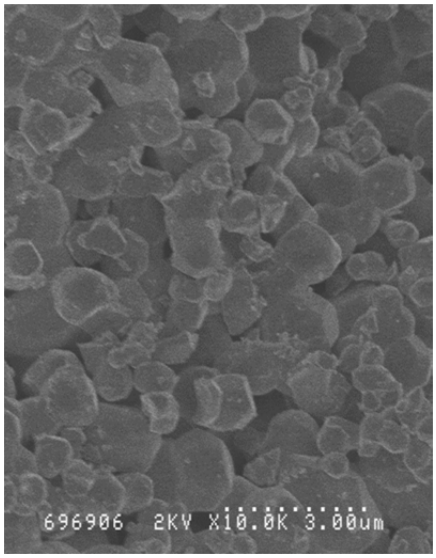

(b) 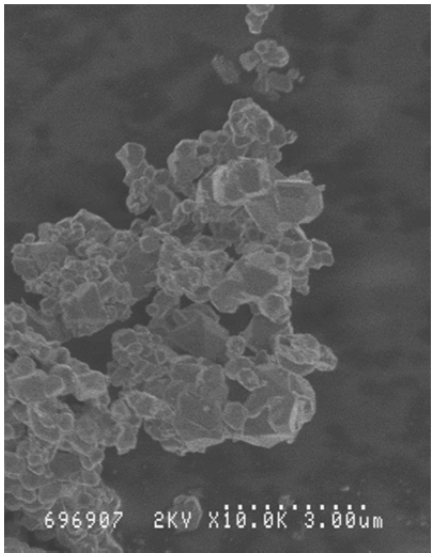

Figure 14. **SEM images of xLi_2MnO_3-(1-x)$Li(CoMnNi)_{0.33}O_2$ comparing temperature and pH control levels with a) moderate control of parameters and b) stringent control of parameters**

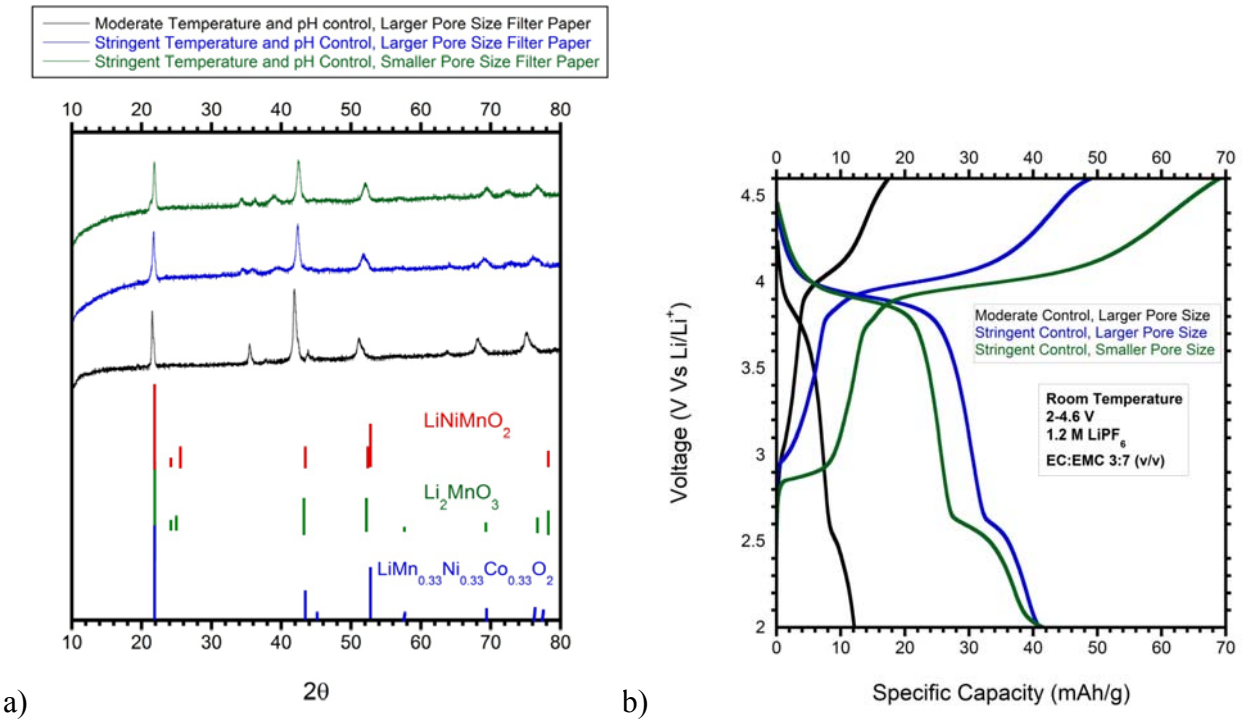

Figure 15. (a) XRD spectra of xLi_2MnO_3-(1-x)$Li(CoMnNi)_{0.33}O_2$ comparing temperature and pH control levels along with type of filter paper used to clean final product. (b) Charge-discharge capacity profiles for xLi_2MnO_3-(1-x)$Li(CoMnNi)_{0.33}O_2$ comparing temperature and pH control levels along with type of filter paper used to clean final product

In addition to SEM, the as-synthesized materials were characterized using XRD to determine if the synthesized material matched the target of Li^2MnO^3-$LiMnCoNiO^2$. A Bruker D2 Phaser benchtop XRD was utilized to scan the candidate samples. Scans ran from $2\theta = 10°$ to 80° using Co Kα radiation as the source. Figure 15(a) presents the XRD patterns for the Li-rich material synthesized under three protocols varying temperature and pH conditions as well as the type of filter paper used during filtration to collect the precipitate. For all three cases, the XRD patterns are in good agreement with the powder diffraction file (PDF) references for all species in the synthesized samples. In the case of the stringent temperature and pH control conditions, it is seen that the material has better agreement with the reference files for the desired product. It is believed that tighter variability during synthesis yields improved quality of the final product.

Electrochemical analysis was performed using 2032 coin cells. Electrodes of the Li-rich material contained 80 wt% active material, 10 wt% PVDF binder, and 10 wt% Super C65 conductive carbon. Coin cells were assembled in an Ar-filled glovebox. The electrolyte prepared was 1.2M $LiPF_6$ EC:EMC (3:7 v/v). Li metal chips were used as the counter electrode in the half cell. All coin cells were cycled galvanostatically between 2V and 4.6V using an Arbin BT-2000 battery cycler. Figure 15(b) shows the charge-discharge capacity profiles for the three previously stated conditions in terms of temperature and pH. Capacity data shows significant improvement in capacity with more rigorous control of temperature and pH; however, additional modifications to synthesis technique required to achieve stated goal.

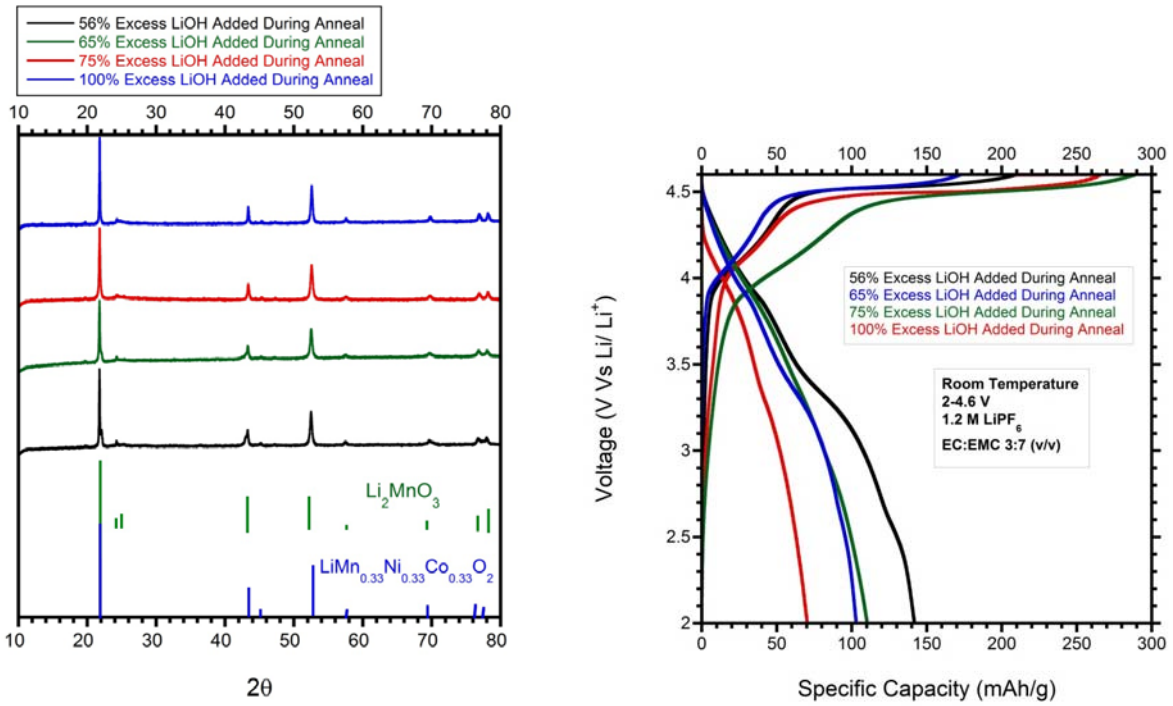

Figure 16. (a) XRD spectra and (b) charge-discharge capacity profiles of xLi_2MnO_3-(1-x)$Li(CoMnNi)_{0.33}O_2$ with varying content of LiOH added during annealing phase of synthesis procedure

To improve the capacity of the as-synthesized material, a study on addition of excess LiOH was undertaken. From previously published experimental protocols, excess LiOH was stated to be necessary during the annealing phase in order to achieve the desired product. Four conditions were studied: 56%, 65%, 75%, and 100% excess LiOH. XRD patterns of the four conditions are shown in Figure 16(a). The XRD patterns are in excellent agreement with the reference patterns for Li_2MnO_3 and $Li(MnNiCo)_{0.33}O_2$ indicating both species are present. Electrochemical charge-discharge capacity results are shown in Figure 16(b). Results indicate that using approximately 56% excess LiOH yields the highest capacity. There exists a transition between adding 75% and 100% excess LiOH, after which the added LiOH will cause an increase in particle size and the presence of amorphous material in the sample. This leads to a significant decrease in capacity performance as shown in Figure 16(b). A significant increase in the active material discharge capacity is realized from this study; however, the highest capacity attained is still below the target of 200 mAh/g.

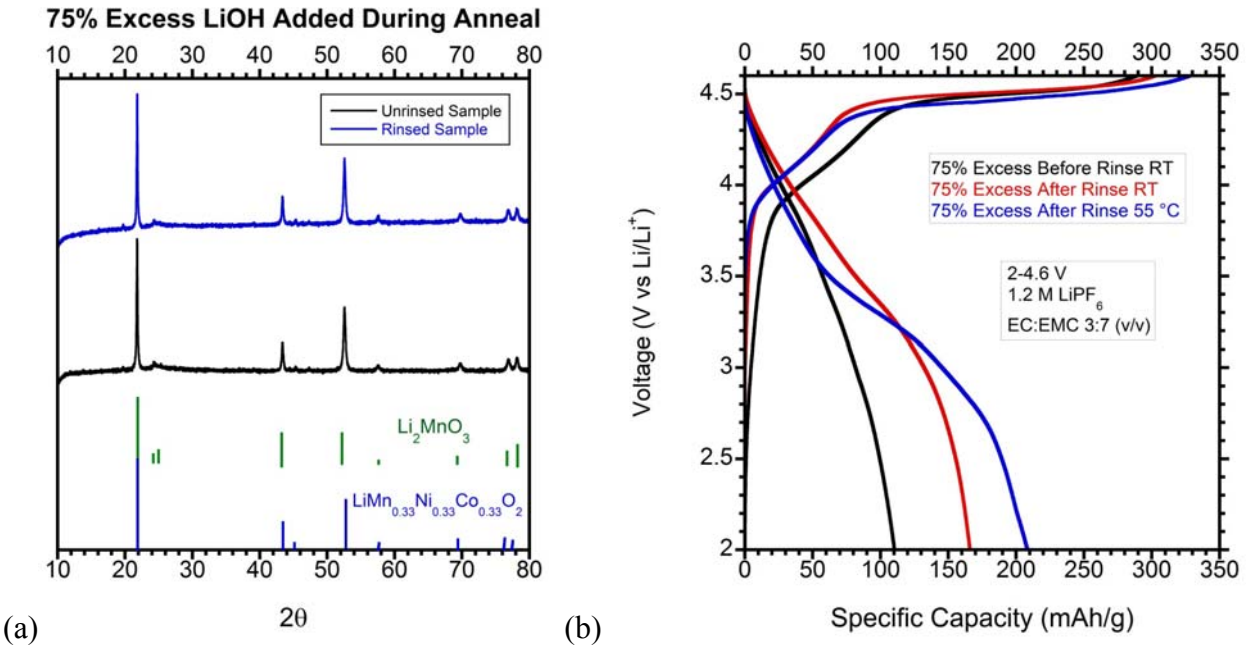

Figure 17. xLi_2MnO_3-(1-x)$Li(CoMnNi)_{0.33}O_2$ synthesized with 75% excess LiOH. (a) XRD spectra comparing material where excess LiOH is rinsed after annealing vs. not rinsed. (b) Charge-discharge capacity profiles for cathode active material before and after rinsing at room temperature and after rinsing electrochemically tested at 55°C

A rinsing study was performed to determine if excess LiOH incorporated during the annealing step actually hindered performance of the active material. Following annealing, the active material was either rinsed with deionized water to remove the excess LiOH or not rinsed. XRD analysis (Figure 17(a)) shows no significant difference between an unrinsed or rinsed sample. Electrochemical testing of the active material under different conditions; however, shows a significant improvement in the capacity. At room temperature, a 50% increase in capacity is attained by rinsing the LiOH after annealing. An additional gain in capacity up to 210 mAh/g is attained when the coin cells are tested under high temperature (55°C) conditions. In both cases, the excess LiOH remaining in the final product acts as impurities, which limits the performance of the cathode. Based on these results, future synthesis will involve rinsing the final product of any excess LiOH prior to characterization.

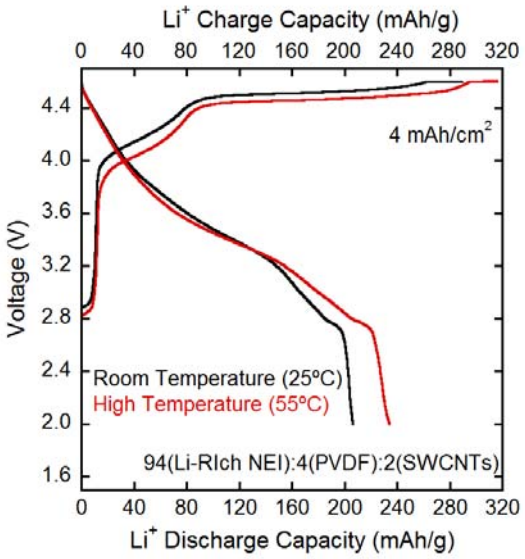

Figure 18. Charge-discharge capacity profiles for NEI Li-rich cathode active material electrochemically tested at 25C and 55C. Composites consisted of replacing traditional conductive carbon with 2 wt% SWCNTs

Commercial Li-rich material obtained from NEI Corporation was tested at room and high temperature conditions. Figure 18 shows the charge-discharge capacity for both cases. Working with NEI commercial Li-rich material, an improvement in capacity is observed when cells tested at 55C with a maximum observable capacity of 240 mAh/g.

5.4 Lithium Rich Microsphere Synthesis

Figure 19(a) is a plot of first cycle charging voltage profiles and Figure 19(b) is a plot of first cycle discharge voltage profiles, where the ethanol evaporation protocol has been varied. It can be observed in Figure 19(b) that direct evaporation of ethanol yielded the best preliminary discharge specific capacity results, with a first cycle discharge capacity of 168 mAh/g at room temperature. This material was also cycled at 55 °C, resulting in a first cycle discharge capacities of 227-235 mAh/g (Figure 20).

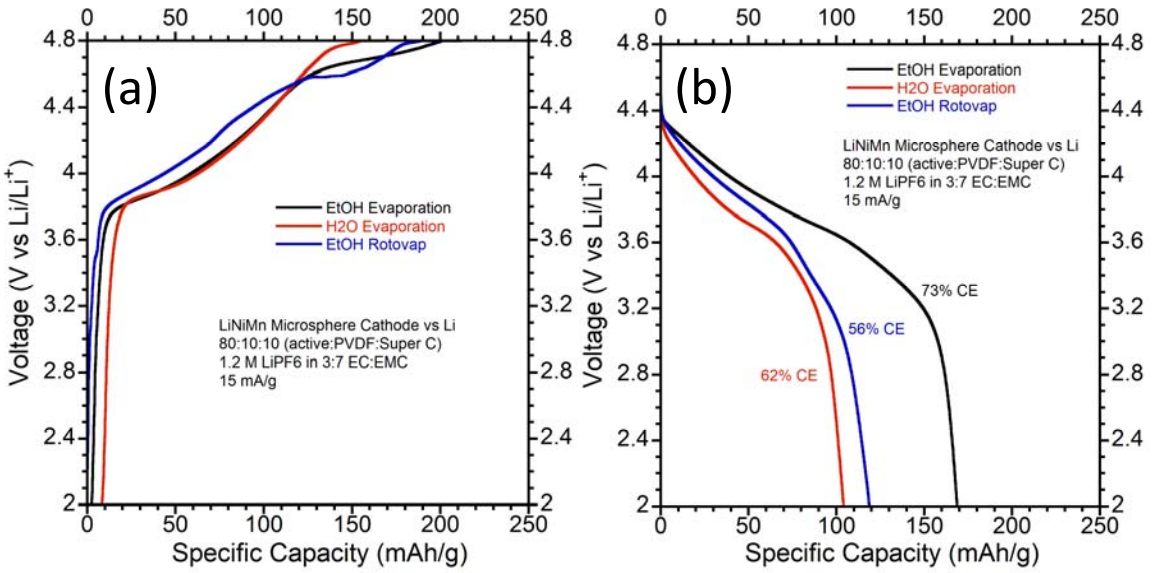

Figure 19. (a) first cycle charging voltage profiles of NPRL synthesized $0.3Li_2MnO_3 \cdot 0.7LiNi_{0.5}Mn_{0.5}O_2$ microspheres final product and (b) discharge profiles

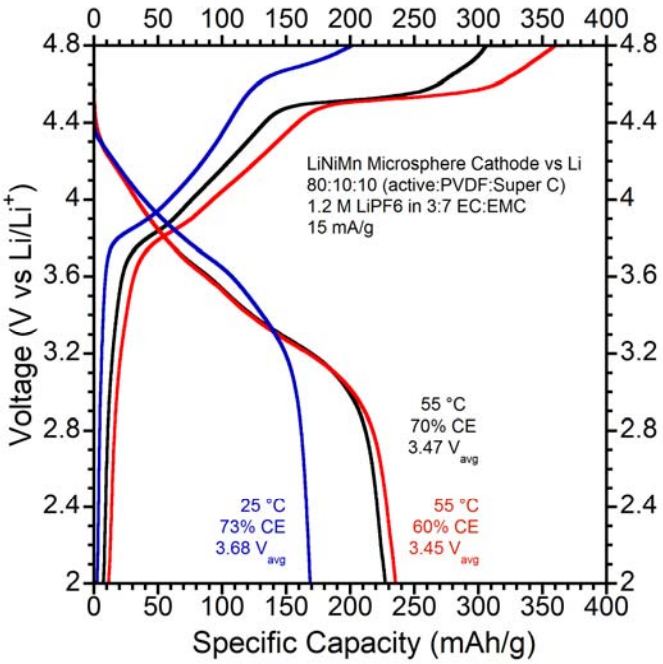

Figure 20. First cycle voltage profiles of LiNiMn microsphere cathodes at 27 °C (blue) and 55 °C (black and red)

5.5 Lithium Rich Cathode on CNTs

A standard composite formulation and additive were used to compare commercial NEI lithium rich cathode material coated on Al and CNT current collectors. The CNT current collector was purified to optimize electrochemical performance. The discharge voltage profiles are shown in Figure 21 at room temperature (25°C). The voltage profile and capacity are slightly lower for the coating on CNTs but is similar to the capacity achieved with CNT additives at low rates and is likely within experimental error.

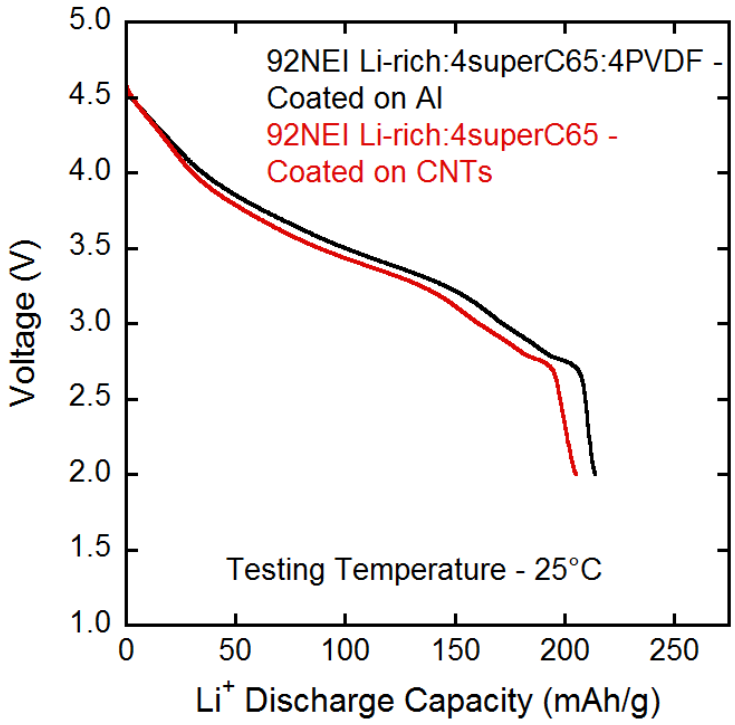

Figure 21. Discharge capacity profiles for NEI Li-rich cathode active material coated on Al and CNTs electrochemically tested at 25°C

The lithium rich coatings on Al and CNTs were tested at high temperature (55°C) as well to investigate the effect of temperature. The voltage profiles are shown in Figure 22 and demonstrate similar voltage profiles with the coating on CNTs having a slightly higher capacity of 248 mAh/g, which is the highest capacity achieved in this work for lithium rich material. Therefore, the lithium rich cathode can be coated onto CNT sheets and has similar electrochemical performance to Al, but with a higher electrode energy density.

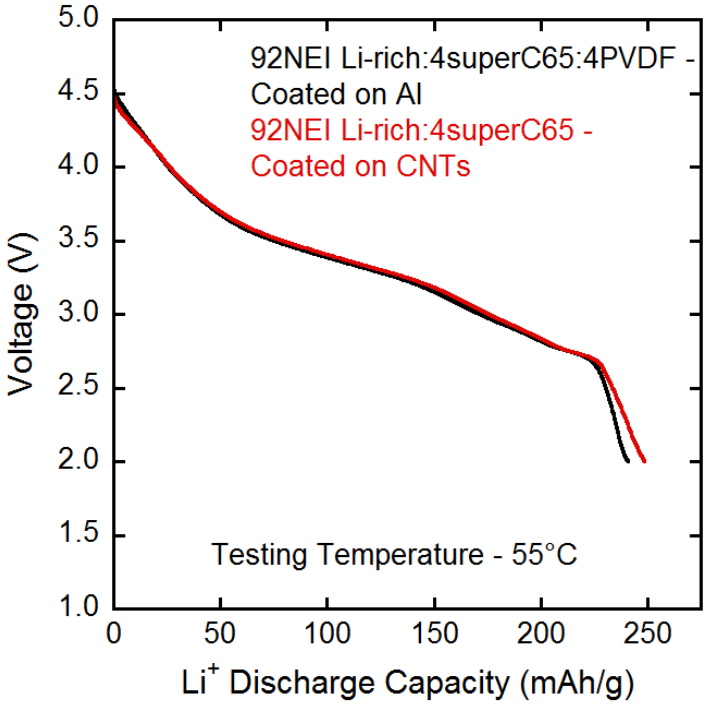

Figure 22. Discharge capacity profiles for NEI Li-rich cathode active material coated on Al and CNTs electrochemically tested at 55°C

The effect of areal capacity, electrode pairing, and temperature on battery energy density was modeled versus a standard MCMB anode. The modeling results are plotted in Figure 23 which demonstrates a larger increase in energy density with higher electrode loadings. Therefore, CNT additives can increase energy density by enabling electrochemical performance at higher areal loadings. The use of a CNT current replacement to Al results in a 10% increase in energy density. A similar increase in energy density is modeled when using a higher capacity lithium rich cathode compared to NCA. The largest increase in energy density is found when going from NCA on Al at room temperature to lithium rich coated on CNTs at high temperature where the energy density increases by approximately 15%.

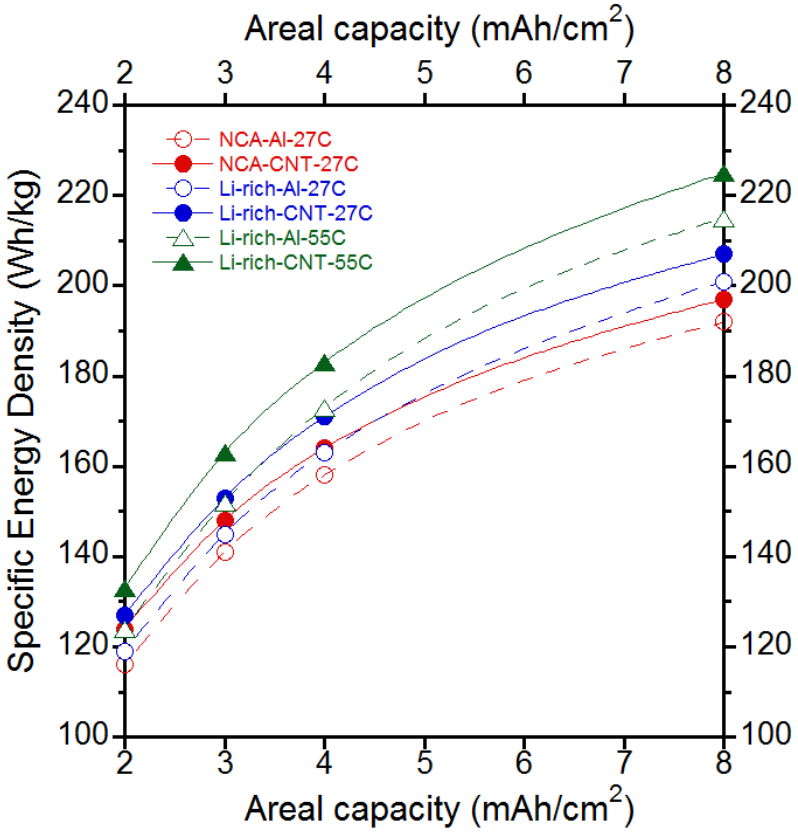

Figure 23. Predicted energy density as a function of electrode pairs within a pouch cell

6.0 CONCLUSIONS

These results demonstrate the ability to coat standard cathode slurries onto CNT papers to enhance energy density, and the importance of CNT purity. Composites coated on purified CNTs had similar performance compared to coatings on metal current collectors. The resulting mass decrease from using CNT supports results in a 5-10% increase in total cell energy density for a battery containing cathode composites on CNTs.

Increased weight loadings of SWCNT additives can significantly improve rate performance of higher areal capacity Li-rich composites compared to traditional composites with carbon black additives. At extremely high loadings (8 mAh/cm^2), increasing additive percentage to 2% weight/weight (w/w) demonstrated equivalent discharge rate performance up to a C/2 rate. At the higher loadings, the rate performance may be further enhanced by optimizing ionic conductivity through controlled electrode porosity. Overall, the SWCNT additives can allow for significantly improved rate performance and higher composite areal loadings which can result in up to a 20-25% increase in battery energy density.

The results from the synthesis of lithium-rich metal oxide cathode materials indicate several factors that must be achieved for successful synthesis and characterization. First, stringent control of synthesis parameters, including temperature and solution pH, must be maintained in

order to avoid wide variability in particle size and performance. Second, tuning the amount of excess LiOH is important to achieve maximum capacity upon testing. Finally, high temperature testing conditions yield the highest capacities and should be investigated further using standard anode materials to properly assess the capabilities of the cathode active material. High capacities achieved were 170 mAh/g at room temperature and 205 mAh/g at 55°C.

Lithium rich microspheres show promise and demonstrate capacities of 170 mAh/g at room temperature and nearly 240 mAh/g at 55°C. Moving forward, several approaches are being evaluated to improve the final product. (1) The initial $MnCO_3$ microsphere synthesis is being modified to increase the microsphere size to 3-5 μm. (2) The effect of ramp rate (1 °C/min vs. 5 °C/min) is being tested for impact on the conversion of $MnCO_3$ to MnO_2. (3) A test matrix of sintering time and temperature during the final synthesis step is being tested with times of 8 hours and 10 hours and temperatures of 800 °C and 1000 °C.

Lithium rich cathode materials coated onto purified CNT current collectors demonstrated equivalent electrochemical performance. The use of higher areal capacities was found to have the largest effect on energy density which was previously shown to be enabled by CNT additives. The use of high capacity lithium rich cathode and CNT current collectors can results in battery energy density increases of 5-15%.

REFERENCES

[1] R. A. DiLeo, *et al.*, "Enhanced Capacity and Rate Capability of Carbon Nanotube Based Anodes with Titanium Contacts for Lithium Ion Batteries," *ACS Nano,* vol. **4**, pp. 6121-6131, 2010/10/26 2010.

[2] S. L. Chou, *et al.*, "Silicon/Single-Walled Carbon Nanotube Composite Paper as a Flexible Anode Material for Lithium Ion Batteries," *The Journal of Physical Chemistry C,* vol. **114**, pp. 15862-15867, 2010/09/23 2010.

[3] J. Alvarenga, *et al.*, "High conductivity carbon nanotube wires from radial densification and ionic doping," *Applied Physics Letters,* vol. **97**, pp. 182106-182106-3, 2010.

[4] P. Jarosz, *et al.*, "Carbon nanotube wires and cables: Near-term applications and future perspectives," *Nanoscale,* vol. **3**, pp. 4542-4553, 2011.

[5] N. Behabtu, *et al.*, "Strong, light, multifunctional fibers of carbon nanotubes with ultrahigh conductivity," *Science,* vol. **339**, pp. 182-186, 2013.

[6] C. S. Johnson, *et al.*, "Anomalous capacity and cycling stability of x Li2MnO3 (1−x) LiMO2 electrodes (M= Mn, Ni, Co) in lithium batteries at 50° C," *Electrochemistry Communications,* vol. **9**, pp. 787-795, 2007.

[7] Y. Jiang, *et al.*, "Hollow 0.3Li2MnO3[middle dot]0.7LiNi0.5Mn0.5O2 microspheres as a high-performance cathode material for lithium-ion batteries," *Physical Chemistry Chemical Physics,* vol. **15**, pp. 2954-2960, 2013.

[8] B. J. Landi, C.D. Cress, C.M. Evans, R.P. Raffaelle, "Thermal Oxidation Profiling of Single-Walled Carbon Nanotubes," *Chem. Mater.,* vol. **17**, pp. 6819-6834, 2005.

[9] M. J. Ganter, *et al.*, "Differential scanning calorimetry analysis of an enhanced LiNi0.8Co0.2O2 cathode with single wall carbon nanotube conductive additives," *Electrochimica Acta,* vol. **56**, pp. 7272-7277, 2011.

LIST OF SYMBOLS, ABBREVIATIONS, AND ACRONYMS

C	C-rate: Unit of current that is equal to the reciprocal of the number of hours for the charge or discharge; e.g. a 1C rate discharge lasts for 1 hour
CNT	carbon nanotube
DI	deionized
DSC	Differential Scanning Calorimetry
EC	ethylene carbonate
EMC	ethyl methyl carbonate
MCMB	mesocarbon microbead
NCA	$LiNiCoAlO_2$ or nickel cobalt aluminum
NMP	N-Methyl-2-pyrrolidone
NPRL	The NanoPower Research Labs
PDF	powder diffraction file
PVDF	polyvinylidene fluoride
SEM	scanning electron microscope
SOA	state of the art
SWCNT	single walled carbon nanotube
w/w	weight/weight
XRD	X-ray diffraction

DISTRIBUTION LIST

DTIC/OCP
8725 John J. Kingman Rd, Suite 0944
Ft Belvoir, VA 22060-6218 1 cy

AFRL/RVIL
Kirtland AFB, NM 87117-5776 2 cys

Official Record Copy
AFRL/RVSV/David Chapman 1 cy

(This page intentionally left blank)